Transition Metal Chemistry
https://doi.org/10.1007/s11243-017-0200-6

A copper(II) complex of 6-(pyrazin-2-yl)-1,3,5-triazine-2,4-diamine and L-serinate: synthesis, crystal structure, DNA-binding and molecular docking studies

Chun-Lian Zhang[1] · Xue-Mei Zhang[1] · Wei Liu[2] · Shi Chen[1] · Xue-Yi Le[1]

Received: 8 October 2017 / Accepted: 20 December 2017

Abstract
A water-soluble Cu(II) complex, $[Cu(pzta)(L\text{-}Ser)(ClO_4)]\cdot 1.5H_2O$ (pzta = 6-(pyrazin-2-yl)-1,3,5-triazine-2,4-diamine; L-Ser = L-serinate), was synthesized and characterized by analytical and spectral techniques. In addition, the molecular structure of the complex was confirmed by single-crystal X-ray diffraction, revealing that the central Cu(II) atom was located in a six-coordinate distorted octahedral geometry. Multi-spectroscopic methods, viscosity measurements and thermal denaturation experiments revealed that the complex binds to DNA with apparent binding constant of $2.93 \times 10^3\ M^{-1}$ through a groove binding mode. The positive values of ΔH and ΔS obtained from isothermal titration calorimetry experiments indicated that hydrophobic interactions play an important role in the formation of the complex–DNA adduct. Molecular docking studies were carried out to better understand the binding mode of the complex with DNA.

Introduction

Over the past few decades, studies of the interactions of metal complexes with nucleic acids have gained much attention because of their relevance in molecular biology and inorganic biochemistry [1, 2]. DNA is an important target in drug discovery, especially for antiviral, anticancer and antibiotic compounds. DNA provides a range of binding sites and modes for covalent and non-covalent interactions including intercalative, electrostatic and groove (surface) binding [3]. A large number of compounds have been reported to bind to DNA, causing DNA damage and influencing the proliferation, transfer and diffusion of cancer cells [4, 5]. Interest in metal complexes that can bind to DNA has been motivated not only by a desire to understand the basics of these interaction modes but also by the development of such complexes into therapeutic agents.

✉ Shi Chen
chens1968@hotmail.com

✉ Xue-Yi Le
lexyfu@163.com

[1] Department of Applied Chemistry, South China Agricultural University, Guangzhou 510642, People's Republic of China

[2] College of Materials and Energy, South China Agricultural University, Guangzhou 510642, People's Republic of China

Platinum-based antitumor drugs like cisplatin, carboplatin and oxaliplatin have been widely used to treat various tumors, but their therapeutic efficacy is nevertheless limited owing to their severe toxicities and susceptibility to drug resistance [6]. Transition metal complexes, with their diverse structural features, redox behavior and physicochemical properties can be useful as therapeutic agents, with low side effects [7]. Amongst the transition metals, Cu(II) complexes with organic ligands have attracted increasing interest because of their biological and pharmaceutical activities that include DNA binding and cleavage, anticancer and antioxidant behaviors, and are considered as promising alternatives to platinum-based drugs [8, 9].

1,3,5-Triazine-substituted derivatives bearing amino groups at positions 2 and 4 have attracted considerable attention due to their chemotherapeutic potential and antiangiogenic properties. In addition, their derivatives can incorporate coordinating groups such as pyridine and pyrazine, whilst the diaminotriazinyl (DAT) group can also engage in supramolecular interactions such as hydrogen bonds [10, 11]. Although metal complexes of 1,3,5-triazine-2,4-diamine derivatives have been reported in the literature, examples with good water solubility are rare [12–14]. Meanwhile, the amino acid L-serine is an excellent ligand for transition metals, which can also bind non-covalently to specific base sequences of DNA via hydrogen bonds between the –OH group of L-serine and the DNA bases [15, 16]. Furthermore,

Published online: 14 February 2018

amino acid/peptide complexes of Cu(II) are of interest, not only for their excellent bioavailability and low toxicity, but also for their potent antitumor and artificial nuclease activities [17–20].

In continuation of our recent studies on Cu(II) complexes of 1,3,5-triazine-2,4-diamine derivatives with amino acid/peptide ligands [18–20], in this paper, a water-soluble Cu(II) complex [Cu(L-Ser)(pzta)(ClO_4)]·1.5H_2O (pzta: 6-(pyrazin-2-yl)-1,3,5-triazine-2,4-diamine; L-Ser: L-serinate) is described. The interaction of the complex with calf thymus DNA (CT-DNA) was investigated by multi-spectroscopic methods (UV, circular dichroism and fluorimetry), as well as viscosity, thermal denaturation and isothermal titration calorimetry (ITC) experiments, plus molecular docking calculations. We have incorporated these experimental and theoretical methods together to explore the binding mode between the Cu(II) complex and DNA, suggesting its application as a potential DNA probe and/or chemotherapeutic agent.

Experimental

Materials and methods

L-Ser and Tris(hydroxymethyl)aminomethane (Tris) were purchased from Sinopharm Chemical Reagent Co., Ltd (China), and used as received. Ethidium bromide (EB) and calf thymus DNA (CT-DNA) were purchased from Sigma (USA). Other materials such as sodium hydroxide, copper(II) perchlorate and solvents (methanol, ethanol and perchloric acid) were of reagent grade. A stock solution of CT-DNA in 5 mM Tris–HCl/50 mM NaCl buffer solution (pH = 7.2) gave a ratio of UV absorbance of 1.8–1.9 at 260 and 280 nm, indicating that the DNA was sufficiently free of protein, and the concentration of DNA was determined by measuring the absorbance at 260 nm using $\varepsilon = 6600\ M^{-1}\ cm^{-1}$ [20]. The synthesized complex used in DNA-binding experiments was directly dissolved in Tris–HCl buffer (pH = 7.2). Deionized water was used to prepare all aqueous solutions throughout the experiments.

IR spectra were recorded using KBr disks (4000–400 cm^{-1}) on a Nicolet ACATAR 360 FTIR spectrometer (Nicolet, USA). Elemental analyses for C, H and N were obtained on a Vario EL elemental analyzer (Elementar, Germany). Molar conductivity was determined using a DDS-11A digital conductometer (Leici, China) in aqueous solution at room temperature. Electrospray mass spectrometry (ESI–MS) was carried out with an API4000 triple quadrupole mass spectrometer (AB Sciex, USA). Fluorescence spectra were recorded with a Hitachi RF-4500 fluorescence spectrometer (Japan). Circular dichroism spectra were measured on a Chirascan CD spectropolarimeter (Applied Photophysics, UK) at room temperature. Isothermal titration calorimetry (ITC) was performed at 25 °C using a VP-ITC isothermal titration calorimeter (MicroCal Inc., Northampton, MA, USA) with a 1.48-mL sample cell and 280-μL titration syringe.

Syntheses

Pzta was synthesized by the reaction of 2-cyanopyrazine with dicyandiamide in 2-methoxyethanol solution as described previously [14]. The Cu(II) complex was obtained by adding a solution of copper(II) perchlorate (0.1853 g, 0.5 mmol) in water (0.5 mL) to a solution of pzta (0.0945 g, 0.5 mmol) in ethanol/water mixed solvent (20 mL, 3/1: v/v). A solution of L-Ser (0.0525 g, 0.5 mmol) treated with NaOH (0.0200 g, 0.5 mmol) was then added dropwise. (Scheme 1) The resulting solution was left to evaporate slowly at room temperature. After a few days, well-shaped crystals suitable for X-ray diffraction were obtained. The product was collected and washed with cold ethanol and water. Yield: 83%. Anal. Calcd for $C_{10}H_{13}ClCuN_8O_7$·1.5H_2O (MW = 475.28) (%): C, 25.27; H, 3.39; N, 23.58. Found (%): C, 25.32; H, 3.19; N, 23.63. IR (KBr, cm^{-1}): ν (OH), 3452 (w), ν_s (NH_2) 3311 (m), ν_{as} (NH_2) 3152 (m), ν (COO^-) 1647 (s), 1384 (m), ν

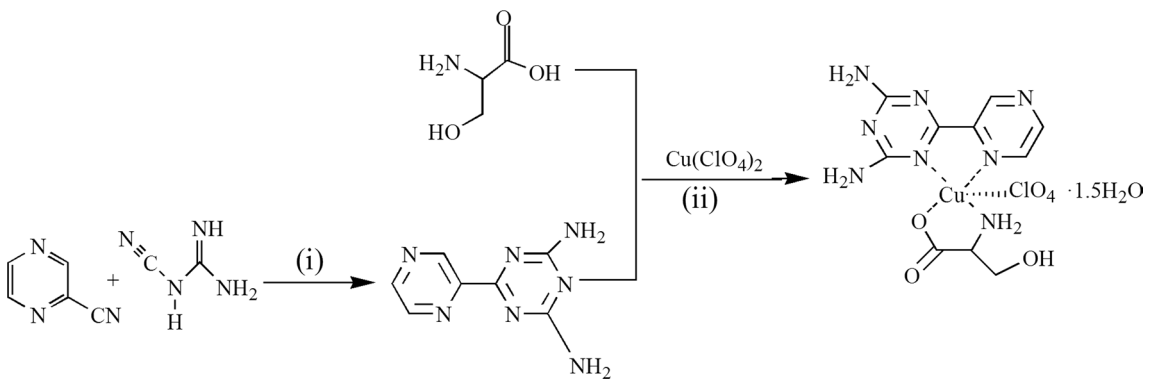

Scheme 1 Synthetic route for the free ligand and its complex. (*i*) $CH_3OCH_2CH_2OH$, KOH, 170 °C, 4 h, (*ii*) EtOH, ca. 60 °C, 2 h

(C=N) 1588 (s). UV–Vis (λ_{max}/nm, ε/M^{-1} cm^{-1}): π–π* 216 (28,795), 279 (8811), d–d 633 (57). Molar conductance, Λ_M (1.0×10^{-3}, H_2O): 109.7 S^{-1} cm^2 mol^{-1} (1:1 electrolyte), ESI–MS (MeOH): $m/z = 356.1$, $[Cu(pzta)(L\text{-}Ser)]^+$.

X-ray crystallographic study

Single-crystal X-ray diffraction measurements of the Cu(II) complex were taken on a Bruker Smart 1000 diffractometer equipped with a CCD area detector at 293 (2) K, using graphite-monochromatized Mo-Kα radiation ($\lambda = 0.71073$ Å) with the φ–ω scan technique. The data were reduced by the SAINT program and corrected for absorption using the semiempirical multi-scan approach (SADABS). The structure was partially solved using direct methods and refined by means of full-matrix least-squares procedures with SHELXL-2014. The hydrogen atoms were added theoretically, and all non-hydrogen atoms were refined anisotropically. The crystallographic data and experimental details of the structure analysis are summarized in Table 1. Selected bond lengths (Å) and angles (°) are given in Table 2. Crystallographic data have been deposited with the Cambridge Crystallographic Data Centre under the accession code CCDC 886547.

Table 1 Crystallographic data and details of refinements for the complex

Empirical formula	$C_{10}H_{13}ClCuN_8O_7 \cdot 1.5H_2O$
Formula weight	475.28
Crystal system	Monoclinic
Temperature (K)	293
λ (Å)	0.71073
Space group	*C*2
a (Å)	14.5540 (3)
b (Å)	6.9698 (14)
c (Å)	16.9620 (3)
β (°)	95.409 (3)
V (Å^3)	1712.9 (6)
Z	4
Dcalc (g/cm^3)	1.839
μ (Mo-Kα) (mm^{-1})	1.494
F (000)	964
Crystal size (mm^3)	$0.11 \times 0.13 \times 0.13$
Refinement method	Full-matrix-least-square on F^2
θ range for date collection (°)	1.2–27.0
Date/parameters/restraints	2800/0/259
Index ranges	$-16 \le h \le 18 - 7 \le k \le 8$ $-21 \le l \le 19$
R (int)	0.018
Goodness of fit on F^2	0.96
Final *R* indices [$I > 2\sigma(I)$]	$R_1 = 0.0275$ $wR_2 = 0.0855$
Flack parameter	0.040(11)

Table 2 Selected bond lengths (Å) and angles (°) for the complex

Bond lengths (Å)			
Cu(1)—O(1)	1.933(2)	Cu(1)—N(1)	1.989(3)
Cu(1)—O(7)	2.479(4)	Cu(1)—N(5)	2.021(3)
Cu(1)—O(5a)	2.467(4)	Cu(1)—N(8)	1.994(3)
Bond angles (°)			
O(1)—Cu(1)—O(7)	89.6(18)	O(7)—Cu(1)—N(8)	92.9(15)
O(1)—Cu(1)—O(5a)	93.46(16)	O(5a)—Cu(1)—N(1)	89.44(17)
O(1)—Cu(1)—N(1)	176.9(2)	O(5a)—Cu(1)—N(5)	82.99(14)
O(1)—Cu(1)—N(5)	97.6(11)	O(5a)—Cu(1)—N(8)	91.01(13)
O(1)—Cu(1)—N(8)	83.4(12)	N(1)—Cu(1)—N(5)	81.5(12)
O(7)—Cu(1)—O(5a)	175.29(14)	N(1)—Cu(1)—N(8)	97.8(13)
O(7)—Cu(1)—N(1)	87.4(19)	N(5)—Cu(1)—N(8)	174.0(3)
O(7)—Cu(1)—N(5)	93.0(17)		

DNA-binding experiments

Absorption titration experiments were carried out by adding CT-DNA at different concentrations (0–17.3 μM) to a fixed concentration of the complex (55 μM). The solutions were left at room temperature for 5 min to ensure complete reaction. The absorption spectra were recorded in the range of 200–400 nm.

The competitive binding study was carried out at constant concentration of EB (4.8 μM) and CT-DNA (5.5 μM) in buffer solution, and increasing the concentrations of the complex from 0 to 40 μM. Emission spectra were recorded in the range of 540–660 nm at room temperature with an excitation wavelength of 591 nm. Before each measurement, the complex–DNA solutions were allowed to incubate for 5 min.

Circular dichroism spectra of CT-DNA (3 mM) were scanned in the range of 200–320 nm by increasing the ratio of [complex] to [CT-DNA] ($r = 0, 0.2, 0.4, 0.6$) in the buffer solution at room temperature, incubating the working solution for 5 min after each addition. The final CD spectrum was generated by averaging three scans and subtracting the buffer background.

Viscosity experiments of CT-DNA were performed in the absence and presence of the complex or EB. The DNA concentration was kept constant (200 μM), and the concentration of the test compound was varied to give [complex]/[DNA] ratios in the range of 0.00–0.30. Flow time was measured with a digital stopwatch. The average time was calculated from triplicate measurements.

DNA thermal denaturation experiments were carried out by monitoring the absorption intensity of CT-DNA (50 μM) at 260 nm in the temperature range from 60 to 100 °C at a scan rate of 1 °C/min, both in the absence and in the

presence of the complex (20 µM). The melting temperature (T_m) of CT-DNA was determined as the transition midpoint.

Isothermal titration calorimetry (ITC) experiments were performed at 25 °C. The buffer solution was degassed thoroughly and then used to prepare all samples. The sample cell was filled with CT-DNA (0.05 mM) solution. The complex (0.2 mM) was sequentially titrated in 25 successive injections of 10 µL under continuous stirring (307 rpm). Ten seconds were taken for each injection, and a time interval of 120 s was set between two consecutive injections to achieve complete equilibration.

Molecular docking

The AutoDock 4.2 program was used to model the interaction between the complex and DNA. The crystal structure of DNA used for the docking study was obtained from the Protein Data Bank with PDB code 1BNA. The X-ray crystal structure of the complex was converted into PDB format using Mercury software. The DNA was prepared for docking by adding polar hydrogens and deleting water molecules. A grid box for the Cu(II) complex and DNA was constructed with 0.375 Å grid spacing. The grid parameters were set to 60, 60 and 60 along the *x*-, *y*- and *z*-axes, respectively, and the grid center was set as $x = 14.719$, $y = 20.979$ and $z = 8.824$ at the site of DNA. For docking calculations, a Lamarckian genetic algorithm (LGA) was implemented with a total of 100 runs for the binding site. In each run, a population of 150 individuals with 27,000 generations and 2,500,000 energy evaluations was employed. After the molecular docking, the output was further analyzed using PyMOL software.

Results and discussion

Synthesis and characterization

The ternary Cu(II) complex was synthesized by reaction of copper(II) perchlorate with pzta and L-Ser in 75% (*v*/*v*) ethanol/H_2O solution. The complex is soluble in water and Tris–HCl buffer (pH = 7.2) solutions. The empirical formula of the complex, as determined by elemental analysis, was confirmed by single-crystal X-ray diffraction. The molar conductance value indicated that the complex is a 1:1 electrolyte in aqueous solution [21]. Its ESI–MS in methanol showed a peak at $m/z = 356.1$, matching exactly with the complex cation $[Cu(pzta)(L\text{-}Ser)]^+$.

In the IR spectrum of the complex, a broad band at 3452 cm^{-1} indicated the presence of water molecules. Two bands at 3311 and 3152 cm^{-1} were ascribed to asymmetric ν_{as} (-NH_2) and symmetric ν_s (–NH_2) stretching vibrations, respectively, of the coordinated and uncoordinated –NH_2 groups. The absence of any band in the range of 1700–1750 cm^{-1} suggested coordination of the COO^- group of L-serinate to the metal. Moreover, the ν_{as} (COO^-) (1647 cm^{-1}) and ν_s (COO^-) (1384 cm^{-1}) stretching frequencies, with $\Delta\nu$ ($\nu_{as} - \nu_s$) value > 200 cm^{-1}, indicated a monodentate coordination mode of the carboxylate groups [22]. The ν (C=N) band of the coordinated pzta (1588 cm^{-1}) was shifted to lower frequencies compared to free pzta (1636 cm^{-1}), consistent with the coordination of the N atom of pzta to the metal. Absorption bands at 640 and 480 cm^{-1} were assigned to the ν (Cu–O) and ν (Cu–N) stretching vibrations, respectively [23].

The electronic spectrum of the complex in aqueous solution showed two strong bands at 216 and 279 nm, which can be attributed to intraligand (π–π^*) transitions of the pzta ligand. A weak and broad band at 633 nm is attributed to the d–d transitions of the Cu(II) metal center [23]. The stability of the complex was studied by UV–Vis spectroscopy in aqueous or Tris–HCl buffer (pH = 7.2) solutions (Fig. 1). The spectra showed virtually no change inabsorbance and wavelength, even after 48 h. These results indicate that the complex is stable in solution under the test conditions for further experiments [24].

Crystal structure of the complex

Single-crystal X-ray diffraction analysis demonstrated that the crystal of the complex belongs to the monoclinic system with space group C2. An ORTEP view of the complex including the atom numbering scheme is shown in Fig. 2. The complex has a polymeric structure assembled from the $[Cu(pzta)(L\text{-}Ser)(ClO_4)]$ unit, where the central Cu(II) atom is located in an octahedral (4 + 1 + 1) CuN_3O_3 geometry. The basal plane is provided by both of the nitrogen atoms (N1, N5) of the pzta ligand plus the nitrogen and oxygen atoms (N8, O1) of the L-Ser co-ligand, whilst the apical positions are occupied by oxygen (O7, O5a) atoms from two perchlorate anions. The trans angles of 176.9° (O1–Cu1–N1) and 174.0° (N5–Cu1–N8) show a small deviation from the expected linear geometry, suggesting distortion in the octahedral coordination geometry. The configurational parameter *t* has a value of 0.05, similar to other related ternary Cu(II)-amino acid/dipeptide complexes [19, 20, 25]. The lengths of the Cu–N/O bonds in the basal plane fall in the range of 1.933–2.021 Å, whilst the bond angles between adjacent coordinating equatorial atoms and the central Cu(II) atom fall in the range of 81.5°–97.8°. The axial oxygen atoms from the perchlorate anions have distances Cu1—O7, 2.479 Å; Cu1—O5a, 2.467 Å that are longer than the equatorial ones, which can be explained by Jahn–Teller distortion [25]. The perchlorate anion generally binds weakly to Cu(II) and tends to be dissociated in solution, similar to the reported complex $[Cu(PyTA)(L\text{-}Thr)(ClO_4)]_2 \cdot 1.5H_2O$ [19].

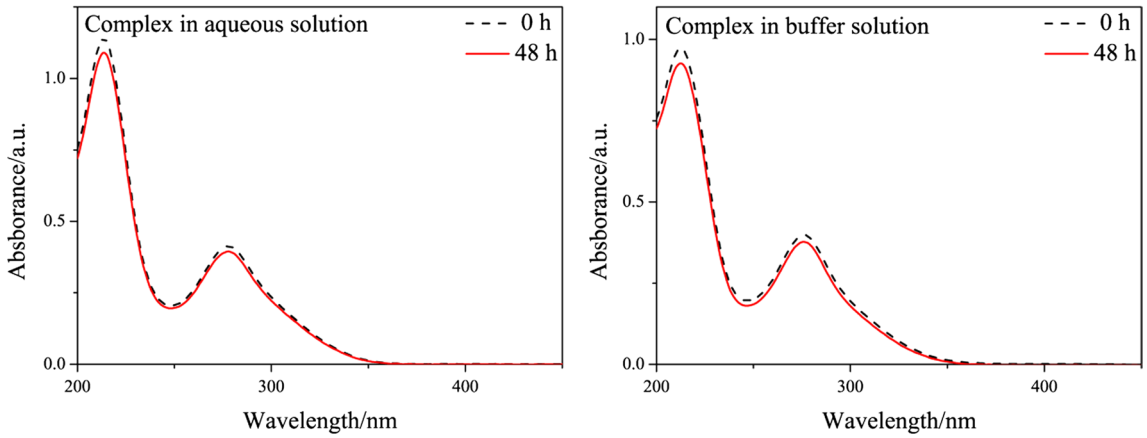

Fig. 1 UV–Vis spectra of the complex in aqueous and Tris–HCl buffer (pH = 7.2) solutions

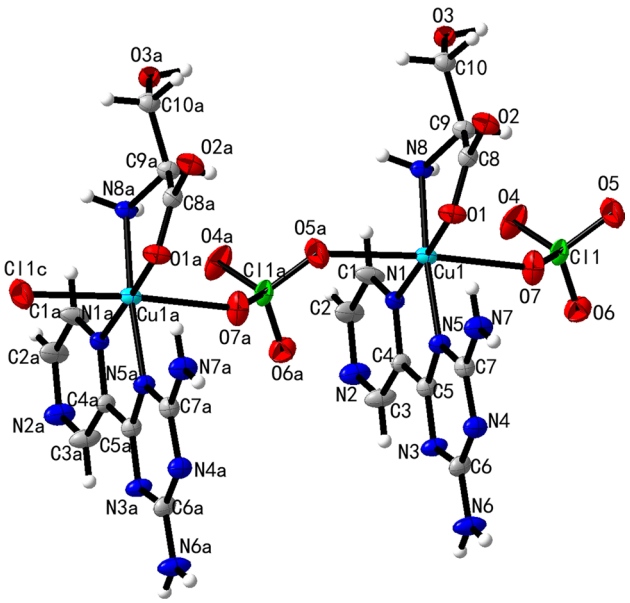

Fig. 2 ORTEP diagram of the complex $[Cu(pzta)(L\text{-}Ser)(ClO_4)]_n$ with the atom labeling scheme

As listed in Table 3, the structure contains a lots of classical N–H···N, N–H···O, N–H···O and non-classical C–H···O hydrogen bonds, in which the uncoordinated NH_2 group of pzta participates in intermolecular hydrogen bonds with the nitrogen atom of the pyrazine ring and one oxygen atom of perchlorate [N6–H6B···N2, 2.965(5) Å and N6–H6A···O6, 3.148(5) Å]. The hydroxyl group of L-Ser forms intermolecular hydrogen bonds with the coordinated NH_2 group and the uncoordinated carboxyl oxygen of another L-Ser [N8–H8B···O3, 3.011(4) Å and O3–H3A···O2, 2.819(5) Å]. In addition, π–π stacking interactions between two neighboring π-systems formed by the $-NH_2$ group and aromatic ring of pzta may play a role in enhancing the crystal stability of the complex. The distance of the nitrogen (NH_2) atom to the centroid of the triazine ring is 3.5 Å, and the stacked planes are approximately parallel to each other (dihedral: 3.1°).

Table 3 Selected hydrogen-bonding interactions for the complex

D-H···A	d(D···A)	< (DHA)
N7-H7B···O1	2.768(4)	154.3
C1-H1…O3[a]	3.134(6)	143.6
N8-H8B…O3[a]	3.011(4)	148.2
C2-H2…O5[b]	3.180(5)	142.7
N6-H6A…O6[c]	3.148(5)	141.5
N6-H6B…N2[d]	2.965(5)	175.9
O3-H3A…O2[e]	2.819(5)	159.1

Symmetry codes: [a] $-x+2, y, -z+1$; [b] $x+1/2, y-1/2, z$; [c] $-x+3/2, y-1/2, -z$; [d] $-x+2, y, -z$; [e] $-x+3/2, y-1/2, -z+1$

DNA-binding experiments

Electronic absorption titrations

Electronic absorption titration is considered to be a reliable method to evaluate the binding affinity of metal complexes with DNA. Upon incremental addition of CT-DNA to the Cu(II) complex, the intensity of its absorption bands decreased (Fig. 3). The observed hypochromic change ($\Delta\varepsilon = 10.24$) without any shift in wavelength suggested that the complex binds to DNA through a groove-binding mode [26]. This hyperchromism can be attributed to van der Waals, hydrophobic and hydrogen-bonding interactions along the major or minor groove of the DNA helix [2]. The intrinsic binding constant (K_b) for the interaction of the complex with CT-DNA was determined from a plot of [DNA]/($\varepsilon_b - \varepsilon_f$) versus [DNA] by means of the equation [27]:

$$[DNA]/(\varepsilon_a - \varepsilon_f) = [DNA]/(\varepsilon_b - \varepsilon_f) + 1/K_b(\varepsilon_b - \varepsilon_f) \quad (1)$$

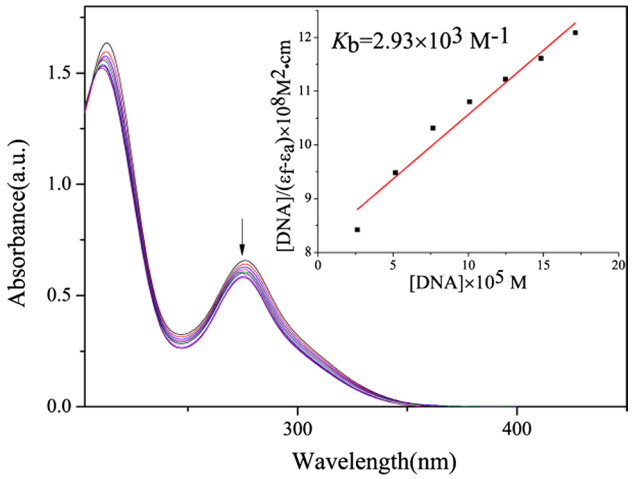

Fig. 3 Absorption spectra of the complex (55 μM) in the absence and presence of increasing concentrations of CT-DNA (0–17.3 μM) at room temperature in Tris–HCl buffer (pH = 7.2)

Here [DNA] is the concentration of the DNA in the base pairs, ε_a is the apparent extinction coefficient obtained by calculating A_{obs}/[complex], and ε_f and ε_b are the extinction coefficient for the free complex and the extinction coefficient for the complex in the fully bound form, respectively. The value of K_b obtained from the ratio of slope to intercept was 2.93 × 10^3 M^{-1}. This is lower than those of some groove binders such as [Cu(PyTA)(L-Thr)(ClO_4)]$_2$·1.5H_2O (6.126 × 10^4 M^{-1}) [19], which might be due to the larger steric hindrance of the pzta ligand [20].

Competitive binding experiments

Competitive binding experiments are used to examine the binding modes of metal complexes with CT-DNA by monitoring the emission intensity of the DNA–ethidium bromide (EB) adduct. EB emits intense fluorescence in the presence of DNA, due to its strong intercalation between adjacent DNA base pairs in the double helix. This fluorescence can be quenched by the addition of a second molecule that can displace the EB [28]. As shown in Fig. 4, the emission intensity of the DNA–EB system at 587 nm was quenched by up to 39.04% with increasing concentrations of the complex, indicating that the complex can compete with EB for DNA binding. A quantitative estimate of this quenching behavior can be obtained by treating the data according to the Stern–Volmer equation [12]:

$$I_0/I = 1 + K_{sq}r \quad (2)$$

where I_0 and I represent the fluorescence intensities of EB–DNA system in the absence and presence of the complex, respectively; r is the concentration ratio of the complex to DNA; and K_{sq} is the Stern–Volmer constant. A plot of I_0/I versus [Q] was linear, and the K_{sq} value was calculated to be 0.19759, which was smaller than those of other reported Cu(II) complexes [29]. It can be concluded that the complex binds to DNA via a groove-binding mode, consistent with the results obtained from the absorption titrations.

Circular dichroism spectra

Circular dichroism (CD) spectroscopy is a versatile tool for detecting any changes of the DNA secondary structure in the presence of metal complexes. The CD spectrum of CT-DNA exhibits a positive band at ~ 275 nm due to base stacking and a negative band at ~ 245 nm due to the right-handed helicity, which is the characteristic of B-DNA [26]. The spectrum shows little or no perturbations in the case of groove binding, but significant changes for intercalation modes [30]. As shown in Fig. 5, in the presence of increasing

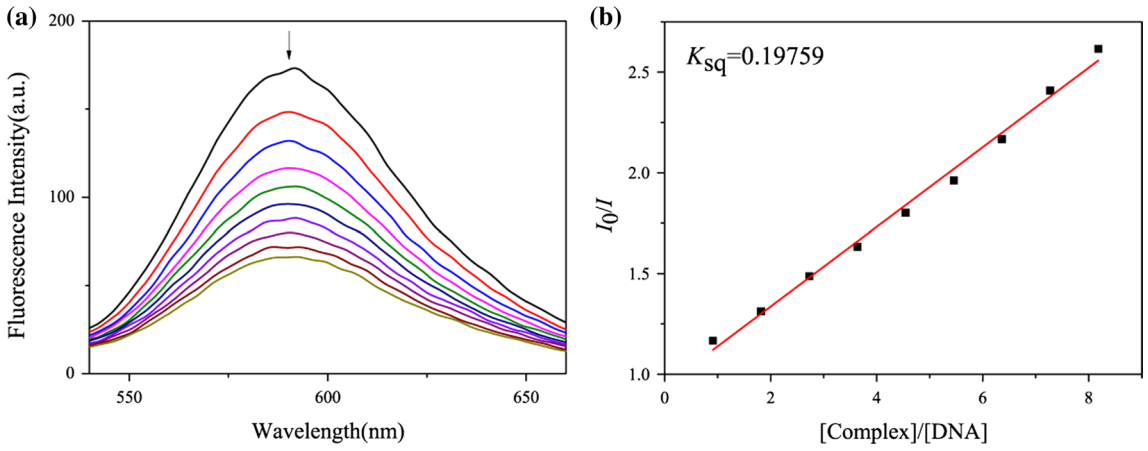

Fig. 4 Left: Emission spectra of EB (4.8 μM) bound to DNA (5.5 μM) in the absence and presence of the complex (0–40 μM) in Tris–HCl buffer (pH = 7.2). Right: Stern–Volmer quenching curve

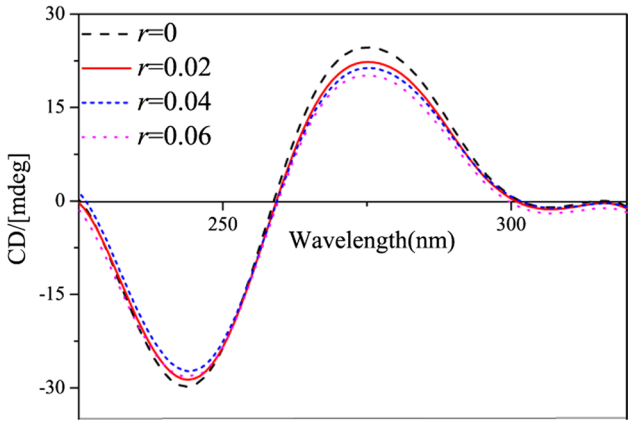

Fig. 5 CD spectra of CT-DNA in the absence and presence of the complex in Tris–HCl buffer (pH = 7.2). Conditions: [DNA] = 200 μM, [Complex]/[DNA] = 0, 0.2, 0.4, 0.6

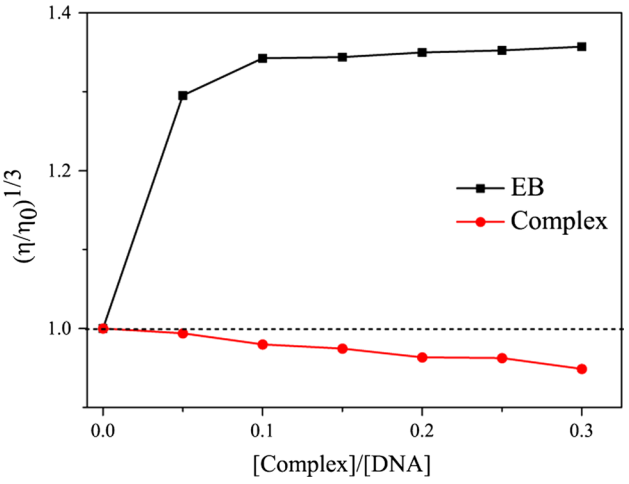

Fig. 6 Effects of increasing EB and the complex on the relative viscosities of CT-DNA at 29 ± 0.1 °C in Tris–HCl buffer (pH = 7.2). Conditions: [DNA] = 200 μM, r = [EB or complex]/[DNA] = 0, 0.05, 0.10, 0.15, 0.20, 0.25, 0.30

concentrations of the complex, no detectable perturbation of the CD spectrum was observed, indicating again that the complex interacts with DNA by a groove-binding mode, in line with the results obtained by electronic absorption and fluorescence spectroscopies.

Viscosity measurements

The DNA-binding mode of metal complexes can also be analyzed by viscosity measurements, since the viscosity of DNA is sensitive to changes in length. The classical intercalative mode causes a significant increase in DNA viscosity, since the base pairs are separated in order to host the bound molecule. In contrast, a small molecule that binds exclusively in the DNA grooves causes little or no change in the viscosity [24]. With this in mind, viscosity measurements were taken, and the results were analyzed as $(\eta/\eta_0)^{1/3}$ versus r, where η and η_0 are the viscosities of DNA in the presence and absence of the complex, respectively, and r is the ratio[complex]/[DNA]. Viscosity values are calculated by the equation:

$$\eta = (t - t_0)/t_0 \quad (3)$$

where t is the flow time of the sample containing CT-DNA, and t_0 is for the buffer alone [23]. As shown in Fig. 6, upon increasing the concentration of the complex, the relative viscosity of DNA decreased steadily, whereas the classical intercalator EB greatly increased the relative viscosity of DNA greatly. These results again suggest that the complex interacts with the groove of DNA.

Thermal denaturation experiments

Thermal denaturation analysis is an important method for the elucidation of DNA-binding mode. When CT-DNA is heated to a certain temperature, the double helix denatures into single strands, which may cause a hyperchromic effect on the absorption spectrum at 260 nm [31]. In general, small molecules that bind to DNA via an intercalation mode increase the denaturation temperature (5–8 °C) due to stabilization of the double-stranded DNA structure, whilst groove-binding molecules give rise to only a small change in denaturation temperature [32]. The melting temperature curves of CT-DNA in the absence and presence of the complex are presented in Fig. 7. The melting temperature (T_m) obtained for free CT-DNA was 79.70 °C and that of the DNA–complex system was 81.54 °C. Such a small change (ΔT_m = 1.84 °C) once again indicates that the complex binds to DNA via a groove-binding mode.

Isothermal titration calorimetry assay

Isothermal titration calorimetry (ITC) provides thermodynamic energetics involved in the binding of a small molecule to a biological macromolecule. This experiment can offer complete thermodynamic profile of the binding; Gibbs free energy (ΔG), enthalpy (ΔH), entropy (ΔS), as well as the number of binding sites (n) and the binding affinity (K_b) [31]. The ITC profile for the binding of the complex to CT-DNA is shown in Fig. 8, in which the upper panel represents the raw ITC curve resulting from the addition of the complex to DNA, whilst the lower panel shows the heats of

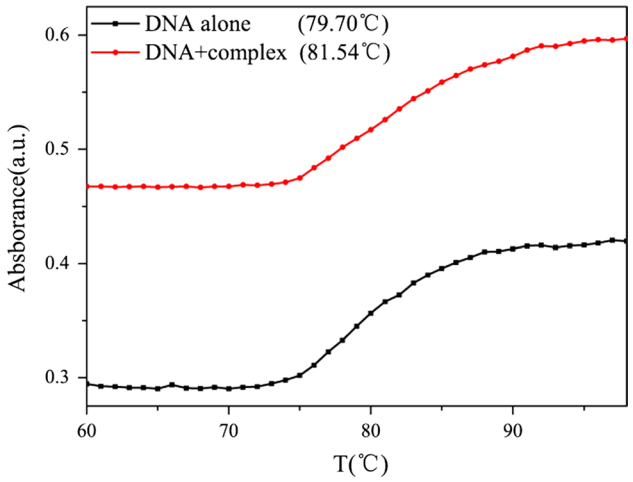

Fig. 7 Thermal denaturation profiles of CT-DNA (50 μM) in Tris–HCl buffer (pH = 7.2) in the absence and presence of the complex (20 μM)

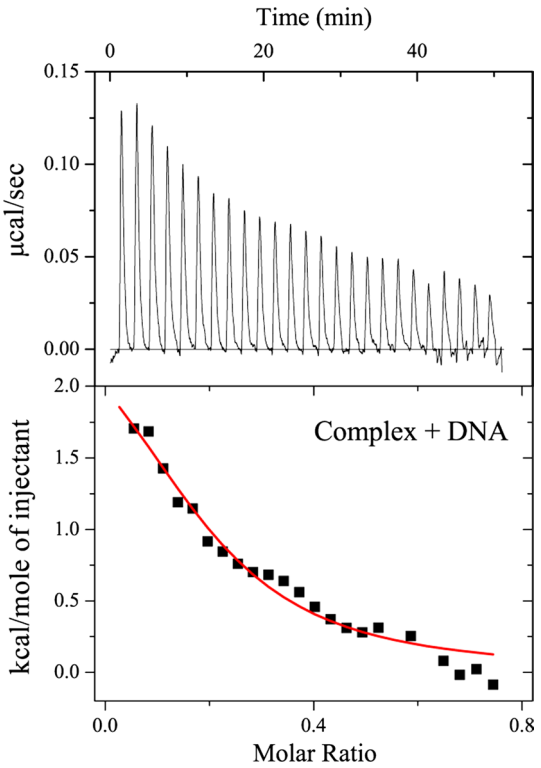

Fig. 8 Isothermal calorimetry titration curves of the complex with CT-DNA in Tris–HCl buffer (pH = 7.2)

reaction plotted against the molar ratio of complex to DNA after the baseline correction. The results show that there is only a single binding mode, with a binding constant of $(1.92 \pm 0.561) \times 10^5\ M^{-1}$, The number of the binding sites was 0.202 ± 0.0302. The thermodynamic parameters such as ΔG, ΔH and ΔS are calculated according to the following equation [32]:

$$\Delta G = \Delta H - T\Delta S \quad (4)$$

This gave values of $\Delta H = 2.908 \pm 0.5784$ kcal/mol, $\Delta G = -7.199$ kcal/mol and $\Delta S = 33.9$ cal/mol. Hence, the binding of the complex to DNA is endothermic, whilst the negative value of ΔG shows that the interaction process is spontaneous. Taken together, the positive values of ΔH and ΔS indicated that hydrophobic interactions play the main role in the binding of the complex to DNA [33].

Molecular docking analysis

Molecular docking software can be used to simulate the binding mode, providing further information on such interaction as an aid in the design of new drugs [34]. The interaction between the complex and DNA was modeled using AutoDock 4.2 program, giving the optimized complex structure shown in Fig. 9a. In this model, the complex is located in the DNA minor groove, and the system is stabilized by various interactions including hydrogen bonds and hydrophobic interactions. As shown in Fig. 9b, the complex is predominantly surrounded by hydrophobic interactions formed by the DNA base pairs of DA15, DA16, DT17, DT28, DT77, DC99 and DG110. Furthermore, two H-bonds were also observed between the complex and DNA with the bond lengths of 2.001 Å (complex: H8B···1-BNA: DT88: O2) and 2.118 Å (complex: H3A···1-BNA: DT88: O4′). The binding energy for the complex–DNA system was −10.37 kcal mol^{-1}, in reasonable agreement with the above experimental data.

Conclusions

A water-soluble Cu(II) complex of 6-(pyrazin-2-yl)-1,3,5-triazine-2,4-diamine and L-Ser has been synthesized and fully characterized. The single-crystal X-ray structure of the complex revealed a slightly distorted octahedral geometry around the central Cu(II) atom. The complex binds to DNA through a groove-binding mode, in which hydrophobic interactions are dominant. This study provides valuable information about the binding mode of the complex with DNA, which may help in the design of better DNA agents for application as nucleic acid molecular probes and new therapeutic reagents for diseases.

Acknowledgements We are grateful to the Program of Guangdong Provincial Science and Technology (2017A020208038) for generous financial support.

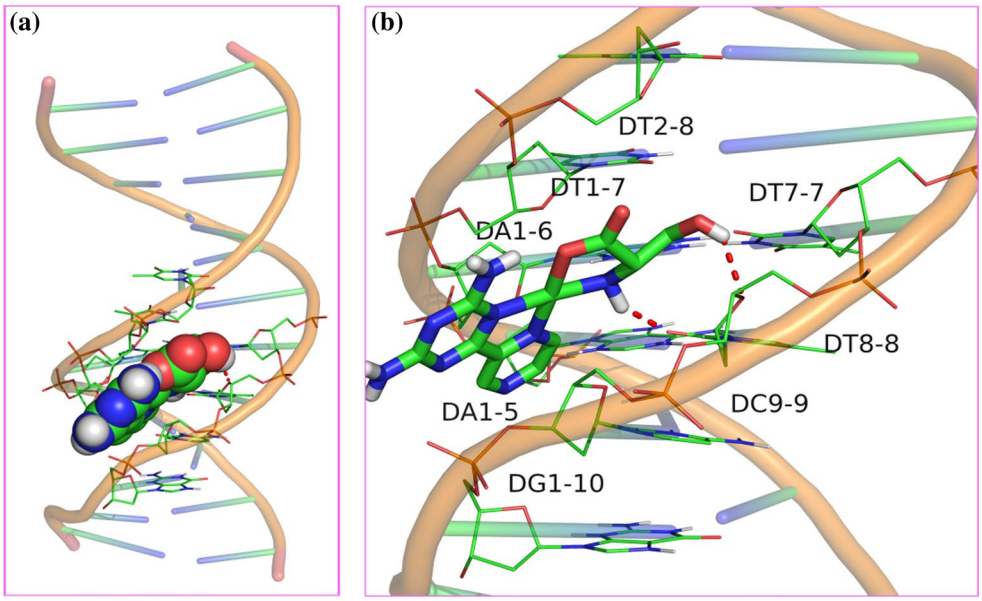

Fig. 9 **a** The molecular docked model of the complex with DNA (1BNA); **b** Detailed view of the docking pose of the complex–DNA system, the hydrogen bonds are represented using red dashed lines

References

1. Jung YW, Lippard SJ (2007) Chem Rev 107:1387–1407
2. Pizarro AM, Sadler PJ (2009) Biochimie 91:1198–1211
3. Brissos RF, Caubet A, Gamez P (2015) Eur J Inorg Chem 2015:2633–2645
4. Deo KM, Pages BJ, Ang DL, Gordon CP, Aldrich-Wright JR (2016) Int J Mol Sci 17:1818–1835
5. Bruijnincx PCA, Sadler PJ (2008) Curr Opin Chem Biol 12:197–206
6. Wheate NJ, Walker S, Craig GE, Oun R (2010) Dalton Trans 39:8113–8127
7. Liang JX, Zhong HJ, Yang GJ, Vellaisamy K, Ma DL, Leung CH (2017) J Inorg Biochem. https://doi.org/10.1016/j.jinorgbio.2017.06.002
8. Marzano C, Pellei M, Tisato F, Santini C (2009) Anti-Cancer Agents Med 9:185–211
9. Santini C, Pellei M, Gandin V, Porchia M, Tisato F, Marzano C (2014) Chem Rev 114:815–862
10. Brzozowski Z, Saczewski F, Gdaniec M (2000) Eur J Med Chem 12:1053–1064
11. Duong A, Metivaud V, Maris T, Wuest JD (2011) Cryst Growth Des 11:2026–2034
12. Duan RR, Wang L, Huo WQ, Chen S, Zhou XH (2014) Spectrochim Acta A 128:614–621
13. Busto N, Valladolid J, Martinez-Alonso M, Lozano HJ, Jalon FA, Manzano BR, Rodriguez AM, Carrion MC, Biver T, Leal JM (2013) Inorg Chem 52:9962–9974
14. Chen Y, Xu WC, Kou JF, Yu BL, Wei XH, Chao H, Ji LN (2010) Inorg Chem Commun 13:1140–1143
15. Micskei K, Patonay T, Caglioti L, Palyi G (2010) Chem Biodivers 7:1660–1669
16. Harada W, Nojima T, Shibayama A, Ueda H, Shindo H, Chikira M (1996) J Inorg Biochem 64:273–285
17. Inci D, Aydın R, Yılmaz D, Gençkal HM, Vatan O, Çinkılıç N, Zorlu Y (2015) Spectrochim Acta A 136:761–770
18. Zhang XM, Ou ZB, Chen S, Xiong YH, Zhou XH, Liu HF, Le XY (2012) J Chin Inorg Chem 28:2667–2673
19. Shen F, Ou ZB, Liu YJ, Liu W, Wang BF, Mao ZW, Le XY (2017) Inorg Chim Acta 465:1–13
20. Fu XB, Liu DD, Lin Y, Hu W, Mao ZW, Le XY (2014) Dalton Trans 43:8721–8737
21. Arjmand F, Aziz M, Chauhan M (2008) J Incl Phenom Macrocycl 61:265–278
22. Chen ZJ, Chen YN, Xu CN, Zhao SS, Cao QY, Qian SS, Qin J, Zhu HL (2016) J Mol Struct 1117:293–299
23. Tabassum S, Amir S, Arjmand F, Pettinari C, Marchetti F, Masciocchi N, Lupidi G, Pettinari R (2013) Eur J Med Chem 60:216–232
24. Lian WJ, Wang XT, Xie CZ, Tian H, Song XQ, Pan HT, Qiao X, Xu JY (2016) Dalton Trans 45:9073–9087
25. Subramanian PS, Suresh E, Dastidar P, Waghmode S, Srinivas D (2001) Inorg Chem 40:4291–4301
26. Xu ZH, Chen FJ, Xi PX, Liu XH, Zeng ZZ (2008) J Photochem Photobiol 196:77–83
27. Pyle AM, Rehmann JP, Meshoyrer R, Kumar CV, Turro NJ, Barton JK (1989) J Am Chem Soc 111:3051–3058
28. Jana SK, Mandal AK, Seth SK, Puschmann H, Hossain M, Dalai S (2016) J Inorg Organomet Polym 26:806–818
29. Liu J, Zhang TX, Lu TB, Qu LH, Zhou H, Zhang QL, Ji LN (2002) J Inorg Biochem 91:269–276
30. Haribabu J, Jeyalakshmi K, Arun Y, Bhuvanesh NSP, Perumalb PT, Karvembu R (2015) RSC Adv 5:46031–46049
31. Rehman SU, Sarwar T, Husain MA, Ishqi HM, Tabish M (2015) Arch Biochem Biophys 576:49–60
32. Ahmad I, Ahmad M (2015) Int J Biol Macromol 79:193–200
33. Xiao Y, Wang Q, Huang YM, Ma XL, Xiong XN, Li H (2016) Dalton Trans 45:10928–10935
34. Ricci CG, Netz PA (2009) J Chem Inf Model 49:1925–1935